# NOISE-INDUCED TRANSITIONS BETWEEN META-STABLE ATMOSPHERIC JETS

TOBIAS GRAFKE

ABSTRACT. We analyze the occurrence of jets in the quasi-linear approximation of the quasi-geostrophic equations in the $\beta$-plane. The occurrence of a time-scale separation between zonal jets and non-zonal turbulent fluctuations gives raise to a law of large numbers, which allows us to compute the meta-stable jet solutions numerically. Similarly, large time-scale separations give raise to a large deviation principle, which in principle gives insight into noise-induced transitions between the fixed points. We use this fact to numerically compute the transition state, i.e. the point at which the noisy dynamics are most likely to cross the separatrix between the respective basins of stability of the deterministic dynamics.

## 1. THE QUASI-GEOSTROPHIC EQUATION IN THE $\beta$-PLANE

We consider 2D stochastically forced barotropic $\beta$-plane turbulence,

$$\partial_t\omega + \vec{v}\cdot\nabla\omega + \beta v = -\lambda\omega - \nu(-\Delta)^p\omega + \sqrt{\gamma}\eta\,, \tag{1}$$

in a periodic domain, $(x,y)\in[0,L]^2$, and where $\vec{v}=(u,v)=e_z\times\nabla\psi$ is the velocity field for a stream function $\psi(x,y)$, $\omega=\Delta\psi$ is the vorticity. Physically, Ekman damping is present with a coefficient $\lambda$, while $\beta$ denotes the local latitude of the planetary surface. Evolving turbulence in this setup transfers energy into zonal shear modes [1] depending on the value of $\beta$, which is the basis of understanding zonal jets in planetary atmospheric dynamics. The forcing $\eta$ is supposed to act only on concentrated modes around the forcing wave number $k_*$ as is common in 2D turbulence [2], but less physically motivated in the atmosphere dynamics case [3]. In particular, we consider $\mathbb{E}\left[\eta(\vec{r}_1,t_1)\eta(\vec{r}_2,t_2)\right]=\delta(t_2-t_1)\chi(|\vec{r}_2-\vec{r}_1|)$.

### 1.1. Rescaling into non-dimensional coordinates.

Following [4], we want to nondimensionalize the parameters. We assume the temporal white noise $\eta$ to be normalized such that $-2\pi^2L^2(\Delta^{-1}\chi)(0)=1$ (since $\eta$ forces vorticity, but energy is measured based on velocity). Consequently, the energy input rate is $\gamma$. Neglecting (hyper-)viscosity, the stationary energy balance yields $E\approx\frac{\gamma}{2\lambda}$.

We now want to rescale to non-dimensional parameters such that the average energy is unity and the domain size is $[0,2\pi]^2$. Define the non-dimensional time $\tau=L^2\sqrt{2\lambda/\gamma}$ and $x'=x/L$, $t'=t/\tau$. Rescale $\omega'=\tau\omega$, $v'=\tau v/L$, $u'=\tau u$, $\beta'=L\tau\beta$ and $\nu'=\nu\tau L^{-2p}$. The forcing correlation has to be rescaled $\chi'(r')=L^4\chi(r)$, and define $\alpha=\tau\lambda$. Inserting

*Date*: October 28, 2016.

all this into equation (1), we arrive at

$$\partial_t\omega + \vec{v}\cdot\nabla\omega + \beta v = -\alpha\omega - \nu(-\Delta)^p\omega + \sqrt{2\alpha}\eta\,, \tag{2}$$

where all primes have been dropped. The forcing pre-factor comes from rescaling time and the spatial forcing correlation as follows: $\sqrt{\gamma}\tau^2(\tau^{-1/2}L^{-2}) = \sqrt{2\alpha}$. We now have reduced the system (1) down to two dimensionless parameters $\alpha, \beta$.

1.2. **Quasi-linear approximation.** A point was made in [4], that the parameter $\alpha$ actually describes a time-scale separation between the slow zonal modes and the fast non-zonal fluctuations. Accordingly, we split vorticity and velocity in equation (2) into zonal and non-zonal components, while assuming a time-scale separation of $\sqrt{\alpha}$ between the zonal mean quantities and the fast fluctuations. More concretely, we set

$$\omega = \Omega + \sqrt{\alpha}\tilde{\omega}, \qquad u = U + \sqrt{\alpha}\tilde{u}, \qquad v = \sqrt{\alpha}\tilde{v}\,, \tag{3}$$

where $\Omega(y) = \frac{1}{L}\int\omega(x,y)\,dx$, $U(y) = \frac{1}{L}\int u(x,y)\,dx$ and $\int v(x,y)\,dx = 0$ because of periodicity. We will drop the tilde in the following and write $\overline{f}$ for averaging over the $x$-coordinate, $\int f(x,y)dx/L$. Inserting (3) into equation (2) and subsequently averaging over $x$, we obtain

$$\partial_t\Omega = -\alpha\overline{v\omega} - \alpha\Omega - \nu(-\partial_y^2)^p\Omega\,.$$

Subtracting this equation from the full one, we obtain an equation for the non-zonal components,

$$\partial_t\omega = -U\partial_x\omega - v\partial_y\Omega - \sqrt{\alpha}\nabla\cdot(\vec{v}\omega) - \alpha\omega - \beta v\,.$$

In the following, we neglect the non-linear interaction term of the non-zonal component. Since $\Omega(y) = -\partial_y U(y)$, we arrive at the quasi-linear approximation

$$\begin{cases}\partial_t U = \alpha\overline{v\omega} - \alpha U - \nu(-\partial_y^2)^p U\\ \partial_t\omega = -U\partial_x\omega - (\partial_y^2 U - \beta)v - \alpha\omega - \nu(-\Delta)^p\omega + \sqrt{2}\eta\,.\end{cases} \tag{4}$$

The kinetic theory of this equation is treated in [4]. Computing the correlation $\mathbb{E}\left[\omega(y_1)\omega(y_2)\right]$ (equivalently, second cumulant) instead of $\omega$ in equation (4), we recover CE2 [5] or equivalently S3T by [6, 7]. This also opens the possibility to analyze emergence and stability of the jets in some detail via linear stability analysis in the context of atmosphere dynamics [8, 9] and in the context of plasma physics [10, 11].

## 2. Meta-stable atmospheric jet solutions and large time-scale separation

It is possible to find parameter ranges in which the quasi-linear approximation (and, hopefully, the fully non-linear system (1)) has multiple stable fixed points of the deterministic dynamics, corresponding to meta-stable jet solutions. In the following, we want to analyze how we compute these fixed points numerically in an efficient way. Furthermore, the limit of large time-scale separation gives raise to a large deviation principle, which allows us to characterize the transition and numerically compute transition states.

2.1. **Large time-scale separation.** The system of equations (4) shows how $\alpha$ can be interpreted as time-scale separation. If we rescale the time by $\alpha$ (and replace the unimportant viscosity $\nu$ with $\alpha\nu$, and $\sigma\sigma^\dagger = \chi$), we obtain

$$\begin{cases} \partial_t U = \overline{v\omega} - U - \nu(-\partial_y^2)^p U \\ d\omega = -\frac{1}{\alpha}\Gamma(U)\omega\, dt + \sqrt{\frac{2}{\alpha}}\sigma dW \end{cases} \tag{5}$$

where the second line is a stochastic PDE and an Ornstein Uhlenbeck process with drift

$$\Gamma(U) = U\partial_x + (\partial_y^2 U - \beta)\partial_x\Delta^{-1} + \alpha + \nu(-\Delta)^p\,. \tag{6}$$

Note that this system, under a suitable discretization, is of the form

$$\dot{X}_i = \sum_{j,k} y_j M_{i,j,k} y_k + RX_i$$
$$dy_j = -\sum_k \Gamma_{j,k} y_k\, dt + \sum_k \sigma_{j,k} dW_k$$

which has the specific form discussed in [12]. In particular, we will make use of the fact that we can write down both a law of large numbers (LLN) and a large deviation principle (LDP) in the limit $\alpha \to 0$.

2.2. **Meta-stable jet configurations.** We want to analyze the meta-stable jet configurations in the limit of large time-scale separation, $\alpha \to 0$. Define the "virtual fast process" $\tilde{\omega}_u$ by

$$d\tilde{\omega}_u = -\Gamma(u)\tilde{\omega}_u + \sqrt{2}\sigma dW\,, \tag{7}$$

i.e. the non-zonal vorticity fluctuations in their natural (fast) time-scale for a fixed zonal velocity $U = u$. Then one can show the existence of an LLN for the mean $\bar{U}$, i.e. $\mathbb{P}(|U(t) - \bar{U}(t)| < \epsilon) \to 1 \forall\, t, \epsilon > 0$ as $\alpha \to 0$. The evolution equation for $\bar{U}(t)$ is given by

$$\begin{aligned} \partial_t \bar{U} &= \mathbb{E}_{\bar{U}}\left[\overline{\tilde{\omega}_{\bar{U}}\tilde{v}_{\bar{U}}}\right] - \bar{U} - \nu(-\Delta)^p\bar{U} \\ &= \frac{1}{L}\int \left(\partial_x\Delta^{-1}\mathbb{E}_{\bar{U}}\left[\tilde{\omega}_{\bar{U}}(x,y)\tilde{\omega}_{\bar{U}}(x',y')\right]\right)_{y=y',x=x'} dx - \bar{U} - \nu(-\Delta)^p\bar{U}\,, \end{aligned} \tag{8}$$

where of course $\tilde{v}_u$ is the velocity corresponding to the virtual fast process. Note that assuming ergodicity we have

$$\mathbb{E}_{\bar{U}}\left[\overline{\tilde{\omega}_{\bar{U}}\tilde{v}_{\bar{U}}}\right] = \lim_{T\to\infty}\frac{1}{T}\int_0^T \overline{\tilde{\omega}_{\bar{U}}\tilde{v}_{\bar{U}}}\, dt\,,$$

which implies that the solution of S3T and CE2 in the large time-scale separation limit converges to the LLN (8).

Since the virtual fast process (7) is an Ornstein-Uhlenbeck process, we can write down its invariant measure explicitly. As a consequence, the correlation matrix of the virtual fast process, $C_{\bar{U}}(x,y,x',y') = \mathbb{E}_{\bar{U}}\left[\tilde{\omega}_{\bar{U}}(x,y)\tilde{\omega}_{\bar{U}}(x,y')\right]$, fulfills the stationary Lyapunov equation

$$\Gamma(\bar{U})C_{\bar{U}} + C_{\bar{U}}\Gamma(\bar{U})^\dagger = 2\sigma\sigma^\dagger\,. \tag{9}$$

We therefore conclude that the zonal dynamics $U$ in the limit of infinite time-scale separation $\alpha \to 0$ can be modeled by the solution $\bar{U}$ of the LLN,

$$\partial_t \bar{U} = \frac{1}{L}\int \left(\partial_x \Delta^{-1} C_{\bar{U}}(x,y,x',y')\right)_{y=y',x=x'} \, dx - \bar{U} - \nu(-\Delta)^p \bar{U} \,, \tag{10}$$

where $C_{\bar{U}}$ is obtained from equation (9).

2.3. **Numerical computation of meta-stable states.** We propose the following algorithm to compute the fixed points of the LLN efficiently. Discretize the $y$-direction with $N_y$ grid points in real space, and the $x$-direction with $N_x$ grid points in Fourier space, defining

$$\omega(x,y) = \sum_{k=-N_x/2}^{N_x/2} \hat{\omega}_k(y) e^{2\pi i k x/L} \,,$$

for the Fourier-coefficients $\hat{\omega}_k(y)$. Since a product in real space is a convolution in Fourier space, and since the mean $\frac{1}{L}\int \cdot \, dx$ is the same as evaluating the $k=0$ coefficient of the Fourier transform, we know that $\overline{v(x,y)\omega(x,y)} = \sum_k \omega_k(y) v_{-k}(y)$. Therefore,

$$\begin{aligned}
\frac{1}{L}\int \left(\partial_x \Delta^{-1} C_{\bar{U}}(y,y')\right)_{y=y',x=x'} \, dx &= \sum_{k=-N_x/2}^{N_x/2} \left(ik(\partial_y^2 - k^2)^{-1} C_k(y,y')\right)_{y=y'} \\
&= \sum_{k=0}^{N_x/2} \left(ik(\partial_y^2 - k^2)^{-1} (C_k(y,y') - C_k^*(y,y')\right)_{y=y'} \\
&= \sum_{k=0}^{N_x/2} \left(-2k(\partial_y^2 - k^2)^{-1} \Im\left[C_k(y,y')\right]\right)_{y=y'} \\
&= \sum_{k=0}^{N_x/2} \mathrm{diag}\left[-2k(\partial_y^2 - k^2)^{-1} \Im\left[C_k(y,y')\right]\right] \,,
\end{aligned}$$

where $\mathrm{diag}[A]$ refers to the main diagonal of the matrix $A$ and $\Im[z]$ is the imaginary part of $z$. The matrix $\Gamma_k(U)$ separates nicely in $k$, so we can solve the Lyapunov equation (9) independently for each $k$, and only for those $k$ where there are forced modes present (otherwise, $\Gamma_k = 0$). In practice, one often considers spatially homogeneous, isotropic forcing around a frequency $k_*$, so that $||\vec{k}| - k_*| < \delta k$ in Fourier space (maybe furthermore restricting not to force the zonal average, $\hat{\chi}(k_x = 0) = 0$). The Lyapunov equation therefore is an equation for matrices of size $n \times n$, which is of computational complexity $\mathcal{O}(n^3)$ [13].

The algorithm we propose in total reads

$$\partial_t U(y) = \sum_{k=0}^{N_x/2} \mathrm{diag}\left[-2k(\partial_y^2 - k^2)^{-1} \Im\left[C_k(y,y')\right]\right] - U(y) - \nu(-\Delta)^p U(y) \tag{11}$$

where for each $t$ and all $k$ the matrix $C_k$ is defined by

$$\Gamma_k(U) C_k + C_k \Gamma_k(U)^\dagger = 2\sigma_k \sigma_k^\dagger \,. \tag{12}$$

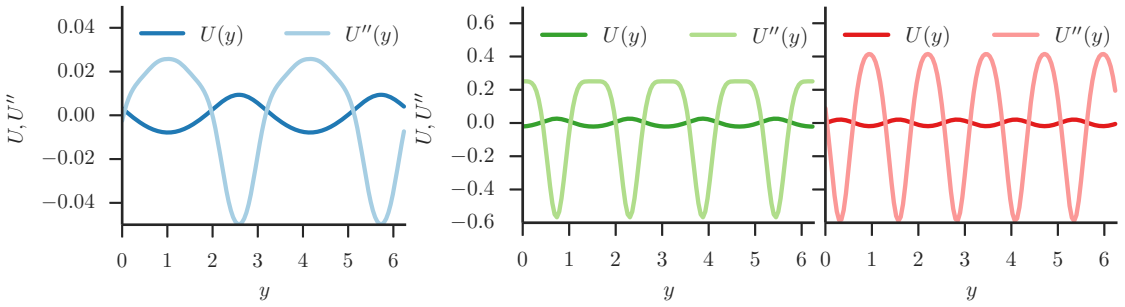


FIGURE 1. Stable configurations for different parameters of $\alpha, \beta$. Left: $\alpha = 10^{-4}, \beta = 1.6$, the 2-jet configuration is the only stable solution. Right: $\alpha = 5 \cdot 10^{-3}, \beta = 5.3$, both 4-jet (green) and 5-jet (red) configurations are stable.

The idea to numerically exploit the separation between macro and micro time scales by decoupling them explicitly is reminiscent of the heterogeneous multiscale method (HMM) [14, 15].

2.4. **Numerical results.** We can use this algorithm as a basis to find sets of parameters $\alpha, \beta$, where the LLN allows multiple stable fixed-points by integrating equation (11) for long times. Note that the integration has to be done only on the slow timescale, i.e. the

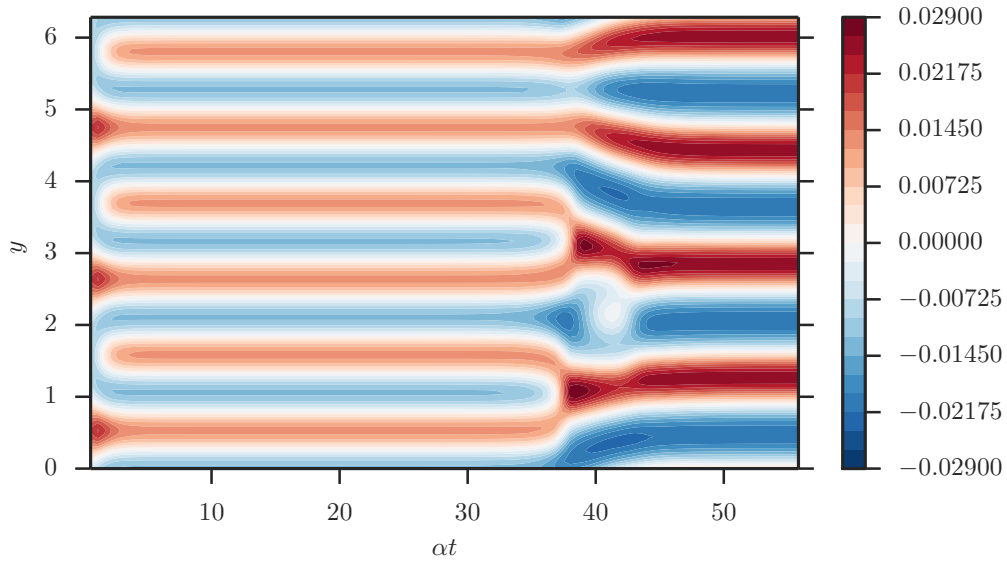


FIGURE 2. Evolution of the LLN equation (8), starting at the (unstable) 3-jet configuration, which eventually evolves into the (stable) 4-jet configuration through a series of splitting and merging events.

fast variable does not limit the numerical stability. Note also that when choosing an unconditionally stable integrator for the (hyper-)viscous term, which poses the strictest stability condition on the relaxation, we can actually view the time integration of (11) as a pre-conditioned iterative descend algorithm to find the fixed point $\partial_t U = 0$. We use exponential time differencing for both linear terms in (11) and obtain the fixed point of the LLN after only a view iterations (time-steps).

In the following, use $N_x = 32$, $N_y = 128$, with a forcing $|\vec{k}| \in [13, 15]$ normalized according to section 1.1 for different values of $\alpha, \beta$. Shown in figure 1 are the meta-stable fixed points of the LLN in which 2 jets (left) and both 4 or 5 jets (right) are stable. Shown in figure 2 is a long-time evolution of the LLN starting at the (unstable) 3-jet configuration, which eventually evolves into the (stable) 4-jet configuration through a series of splitting and merging events. Note that in this evolution, it is always the retrograde jets that split, and always the prograde jets that merge.

## 3. Noise-induced transitions between meta-stable jet configurations

The computation of the full large deviation minimizers for the transition trajectories is complicated. As indicated in [12], there is no explicit formula for the large deviation Hamiltonian of the complete system. However, we can gain some insight into the merging events by computing the heteroclinic orbit connecting different meta-stable states. In particular, this allows a computation of the transition state (saddle point) which must also be part of the transition trajectory, as well as the downhill trajectory onwards from there. This implies that we get access to the configuration at which the separatrix between the basins of attraction of the respective fixed points is most likely crossed in the limit $\alpha \to 0$.

### 3.1. **Transition state and heteroclinic orbit.**

The heteroclinic orbit can be computed via the string method [16] by integrating the LLN equation (8) for several images along a string connecting the meta-stable states, while simultaneously keeping the string artificially arc-length parametrized. More precisely, consider a family of configurations $U_s(y)$ parametrized by $s \in [0, 1]$, such that $U_0$ and $U_1$ are two stable fixed points of the LLN equation (8). Then, relax the string $U_s$ in virtual time $\tau$ by

$$\partial_\tau U_s = (1 - \hat{t} \otimes \hat{t}) b(U_s)\,, \tag{13}$$

where $\hat{t} = \partial_s U_s / |\partial_s U_s|$ is the unit tangent vector along the string, $(1 - \hat{t} \otimes \hat{t})$ is the projector on the component perpendicular to the string at each point, and

$$b(U_s) = \mathbb{E}_{U_s}\left[\widetilde{\omega_{U_s} \tilde{v}_{U_s}}\right] - U_s - \nu(-\Delta)^p U_s$$

is the dynamics of the averaged zonal velocity. When converged, this ensures that at each point $s$ along the string we have $\partial_s U_s \parallel b(U_s)$ and $U_s$ is the heteroclinic orbit connecting the two stable fixed points with a saddle-point in-between. In particular, this orbit contains the saddle point configuration $\hat{U} = U_{\hat{s}}$, $\hat{s} \in (0, 1)$ where the dynamics vanish, $b(\hat{U}) = 0$ and the only unstable direction is tangential to the string. This saddle point also has to be contained in the minimizer (or at least a local minimizer) of the rate function (which we don't have access to) and corresponds to the point at which the separatrix between the basins of stability of the LLN equation is crossed.

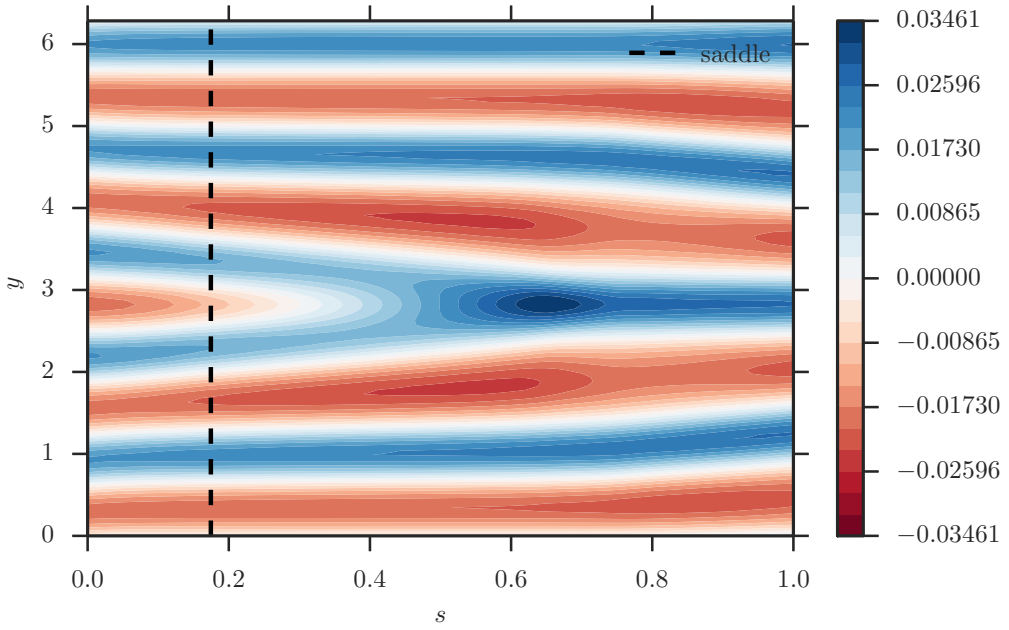


FIGURE 3. Heteroclinic orbit connecting the meta-stable 5-jet configuration $U_5$ to the meta-stable 4-jet configuration $U_4$. The saddle $\hat{U}$ is located at approximately $\hat{s} \approx 0.17$.

Note that this procedure does not allow an estimate of the relative stability of the configurations, the transition probabilities or the exit times. We can use the saddle-point calculation to reduce the complexity of the full minimization somewhat, though, by only requiring a computation of the "uphill" trajectory up to the saddle point.

3.2. **Numerical computation of the transition state and heteroclinic orbit.** Numerically, one has to solve the Lyapunov equation (9) for each $k$ and each image along the string until the iteration reaches a fixed point. The projection on the component perpendicular to the string is most easily implemented by reparametrization after every iteration.

As example case, we take the parameters $\alpha = 5 \cdot 10^{-3}, \beta = 5.3$ which exhibit locally stable 4- and 5-jet configurations as shown in figure 1 (right). The heteroclinic orbit connecting these two configurations $U_4$ and $U_5$ is shown in figure 3. Here, $s \in [0, 1]$ denotes the string parameter, with $U(s = 0) = U_5$ and $U(s = 1) = U_4$. The corresponding saddle point configuration can be identified at roughly $\hat{s} \approx 0.17$, where $b(\hat{U})$ close to zero. It is depicted in figure 4 in comparison to $U_5$.

Note that in contrast to the results of Bouchet and Simonnet [17] I am only able to find a single saddle point, namely the one where a prograde jet merges/splits, not the one where a retrograde merges/splits. This is regardless of the initial condition from which the string relaxes, and in particular also applies to the case where I intentionally start with a retrograde split initial condition. In contrast, the results obtained from adaptive multilevel splitting (AMS) [17] seem to suggest that forward- and backward transition appear to split retrograde jets, but merge prograde jets (which is in agreement with the

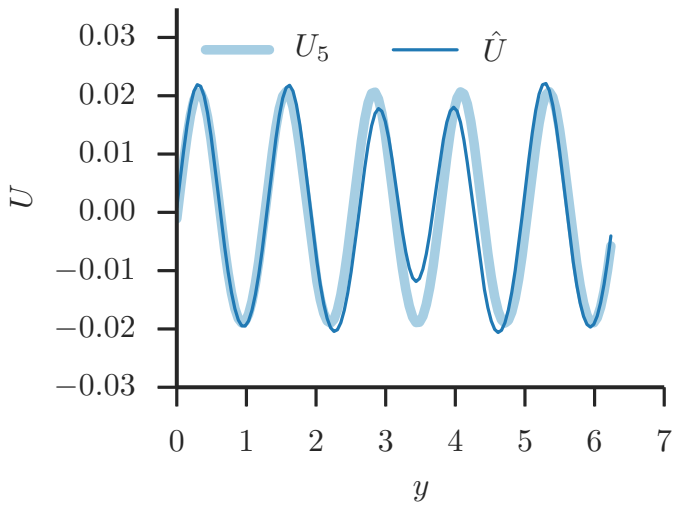


FIGURE 4. Saddle point configuration $\hat{U}$ in comparison to the 5-jet configuration $U_5$.

deterministic behavior of section 2.4), and the transition trajectories share no points except the equilibria. It is not clear whether this points to a systematic difference or is simply the consequence of different parameters. The location of the saddle points in the AMS simulations is somewhat unclear, as well.

The numerical parameters are $N_x = 32, N_y = 128$ for each image, with $N_{\text{images}} = 128$ and a number of iterations of roughly $N_{\text{iter}} \approx 10^2$.

## REFERENCES

[1] Peter B. Rhines. Waves and turbulence on a beta-plane. *Journal of Fluid Mechanics*, 69(03):417–443, June 1975. ISSN 1469-7645. doi:10.1017/S0022112075001504.

[2] Douglas K. Lilly. Numerical Simulation of Two-dimensional Turbulence. *Physics of Fluids (1958-1988)*, 12(12):II–240–II–249, December 1969. ISSN 0031-9171. doi:10.1063/1.1692444.

[3] Kaushik Srinivasan and W. R. Young. Zonostrophic Instability. *Journal of the Atmospheric Sciences*, 69(5):1633–1656, December 2011. ISSN 0022-4928. doi:10.1175/JAS-D-11-0200.1.

[4] Freddy Bouchet, Cesare Nardini, and Tomás Tangarife. Kinetic Theory of Jet Dynamics in the Stochastic Barotropic and 2d Navier-Stokes Equations. *Journal of Statistical Physics*, 153(4):572–625, September 2013. ISSN 0022-4715, 1572-9613. doi:10.1007/s10955-013-0828-3.

[5] J. B. Marston, E. Conover, and Tapio Schneider. Statistics of an Unstable Barotropic Jet from a Cumulant Expansion. *Journal of the Atmospheric Sciences*, 65(6):1955–1966, June 2008. ISSN 0022-4928. doi:10.1175/2007JAS2510.1.

[6] Brian F. Farrell and Petros J. Ioannou. Structural Stability of Turbulent Jets. *Journal of the Atmospheric Sciences*, 60(17):2101–2118, September 2003. ISSN 0022-4928. doi:10.1175/1520-0469(2003)060<2101:SSOTJ>2.0.CO;2.

[7] Brian F. Farrell and Petros J. Ioannou. Structure and Spacing of Jets in Barotropic Turbulence. *Journal of the Atmospheric Sciences*, 64(10):3652–3665, October 2007. ISSN 0022-4928. doi:10.1175/JAS4016.1.

[8] Nikolaos A. Bakas and Petros J. Ioannou. Structural stability theory of two-dimensional fluid flow under stochastic forcing. *Journal of Fluid Mechanics*, 682: 332–361, September 2011. ISSN 1469-7645. doi:10.1017/jfm.2011.228.

[9] Nikolaos A. Bakas and Petros J. Ioannou. Emergence of Large Scale Structure in Barotropic $\beta$-Plane Turbulence. *Physical Review Letters*, 110(22):224501, May 2013. doi:10.1103/PhysRevLett.110.224501.

[10] Jeffrey B. Parker and John A. Krommes. Zonal flow as pattern formation. *Physics of Plasmas (1994-present)*, 20(10):100703, October 2013. ISSN 1070-664X, 1089-7674. doi:10.1063/1.4828717.

[11] Jeffrey B. Parker and John A. Krommes. Generation of zonal flows through symmetry breaking of statistical homogeneity. *New Journal of Physics*, 16(3):035006, March 2014. ISSN 1367-2630. doi:10.1088/1367-2630/16/3/035006.

[12] Freddy Bouchet, Tobias Grafke, TomÃ¡s Tangarife, and Eric Vanden-Eijnden. Large Deviations in Fast-Slow Systems. *Journal of Statistical Physics*, pages 1–20, January 2016. ISSN 0022-4715, 1572-9613. doi:10.1007/s10955-016-1449-4.

[13] R. H. Bartels and G. W. Stewart. Solution of the Matrix Equation AX + XB = C [F4]. *Commun. ACM*, 15(9):820–826, September 1972. ISSN 0001-0782. doi:10.1145/361573.361582.

[14] Weinan E, Björn Engquist, and Zhongyi Huang. Heterogeneous multiscale method: A general methodology for multiscale modeling. *Physical Review B*, 67(9):092101, March 2003. doi:10.1103/PhysRevB.67.092101.

[15] Weinan E, Björn Engquist, Xiantao Li, Weiqing Ren, and Eric Vanden-Eijnden. Heterogeneous multiscale methods : A review. *Communications in Computational Physics*, 2(3):367–450, 2007.

[16] Weinan E, Weiqing Ren, and Eric Vanden-Eijnden. String method for the study of rare events. *Physical Review B*, 66(5):052301, August 2002. doi:10.1103/PhysRevB.66.052301.

[17] Freddy Bouchet and Eric Simonnet. Geostrophic jet transitions from the adaptive multilevel splitting algorithm. private communication, 2016.